ChemComm

COMMUNICATION

View Article Online
View Journal | View Issue

Cite this: *Chem. Commun.*, 2015, **51**, 11190

Received 21st May 2015,
Accepted 9th June 2015

DOI: 10.1039/c5cc04120a

www.rsc.org/chemcomm

Micromotor-based on–off fluorescence detection of sarin and soman simulants†

Virendra V. Singh, Kevin Kaufmann, Jahir Orozco, Jinxing Li, Michael Galarnyk, Gaurav Arya and Joseph Wang*

Self-propelled micromotor-based fluorescent "*On–Off*" detection of nerve agents is described. The motion-based assay utilizes Si/Pt Janus micromotors coated with fluoresceinamine toward real-time "*on-the-fly*" field detection of sarin and soman simulants.

Chemical warfare agents (CWA) are some of the most nefarious weapons of mass destruction.[1] The ease of manufacturing and dispensability, ease of availability, and inexpensive starting materials make them an eminent global threat.[1] Nerve agents are a particularly dangerous class of CWA that continue to be a threat in spite of controls imposed by the chemical weapon convention (CWC) which prohibits the production and use of chemicals on enemy forces.[2,3] Their rapid and severe effects on human health stem from their ability to irreversibly inhibit acetylcholinesterase activity by phosphorylation and leads to neuromuscular paralysis and eventually death.[4–6] A particularly dangerous class of organophosphorus nerve agents is the phosphoryl fluoride containing species such as sarin and soman,[7–9] referred to as GB and GD agents, respectively. Unfortunately, these highly reactive and volatile nerve agents are colorless, odorless, and tasteless, making their detection very difficult. Therefore, a reliable and rapid nerve agent detection system is highly desirable amidst the current climate of terrorism awareness. Among a variety of detection methods that have been developed for these nerve agents,[9] fluorescent detection offers the unrivaled merits of high sensitivity, low-cost and operational simplicity.[10–12] The chromo-fluorogenic detection is especially attractive because it allows simple visual detection *in situ*, or on-site, without any sample pretreatment or the use of complex equipment.[10–12] As a result, the development of highly sensitive, selective, ready-to-use, and rapid field screening methods for these nerve agents has become an increasingly imperative research goal.

Herein we demonstrate an extremely fast (~10 s) fluorescent "*On–Off*" detection of sarin and soman simulants based on self-propelled dye-coated micromotors. Artificial/synthetic micromotors have recently attracted considerable interest due to their attractive capabilities and diverse potential applications, ranging from directed drug delivery to environmental detection.[13–15] The self-propulsion capability of micromotors induces efficient fluid mixing, a very useful property for environments that would not allow mechanical agitation (*i.e.*, bodies of water, stealthy national defense operations, *etc.*) or at the microscale level. This motor-induced mixing has shown to be extremely effective in accelerating both target–receptor interaction,[13–15] detection,[16,17] and detoxification reactions.[18–20] Recently, there has been a considerable interest in micromotor-based defenses against chemical and biological warfare agents;[18–20] these include the potential use of functionalized micromotors as efficient screening tools for the real time and on-site detection of chemical threats in environmental matrices.

Fluorescence quenching methods have been emerging as an effective route for sensitive and low cost field detection.[21–23] In this regard, fluorescent 'turn-off' based sensors have been developed for nitrated explosive compounds[22] and Hg^{2+}.[23] Such 'turn-off' sensors have shown to be more sensitive than their 'turn-on' sensor counterpart.[22,23] The motion-based accelerated nerve-agent detection, described in the presence work and illustrated in Fig. 1, relies on coating catalytic microsphere micromotors with the fluorophore fluoresceinamine (FLA) that reacts quickly with phosphoryl halides.[24] Diethyl chlorophosphate (DCP) is used as a nerve agent simulant as it has similar reactivity of common nerve agents, yet lacks their potent efficacy and related safety concerns (Fig. S1, ESI†).[12]

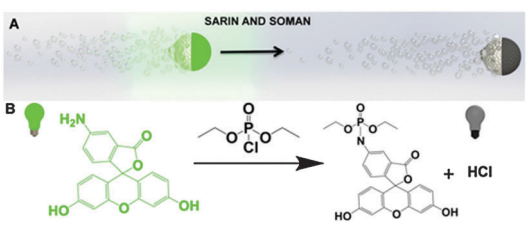

Fig. 1 Schematic representation of the micromotor based *'on-the-fly'* fluorescent *"On–Off"* detection of nerve agent and (B) reaction mechanism showing the reaction of FLA coated micromotor with DCP.

Department of Nanoengineering, University of California San Diego, La Jolla, CA 92093, USA. E-mail: josephwang@ucsd.edu

† Electronic supplementary information (ESI) available. See DOI: 10.1039/c5cc04120a

Microbead chemical switches were shown to be useful for detecting reactive organophosphate CWA vapors using buffers and appropriate proton scavengers.[25] Moreover, it was also found that fluorescence intensity increased first and then decreased over time which may lead to false positive fluorescent "*Off–On*" detection. However, since in the field conditions, the concentration of CWA and other metrological conditions are often unknown, the detection of CWA in natural water matrices is more challenging compared to vapor measurements since proper buffering and a suitable proton scavenger are very important. To date, this has made the detection process unfeasible. As will be illustrated below, the new micromotor strategy addresses these challenges toward rapid fluorescent "*On–Off*" route for instantaneous detection of sarin and soman simulants.

The self-propulsion capability of the dye-coated micromotors, along with the corresponding bubble tail, are shown to generate effective fluid convection (without external force) that results in an increased rate of collision between the micromotors and the target nerve agent, thereby offering a rapid '*on-the-fly*' fluorescent "*On–Off*" detection method. The fluid mixing capability of micromotors[26] has been used recently for accelerated environmental remediation and detoxification processes.[18–20] Similarly, the efficient movement of the FLA-coated microsphere, along with the substantial fluid transport, are used in the following sections for developing an attractive "*On–Off*" CWA detection approach.

As illustrated in Fig. 1A, self-propelled FLA/silica–NH_2/Pt micromotors perform "*on-the-fly*" fluorescent detection of nerve agents in environmental matrices. Fig. 1B displays the reaction mechanism involving the FLA/silica–NH_2/Pt micromotor and nerve agent. These micromotors, along with inherent efficient solution mixing, resulted in the dramatic quenching of FLA fluorescence upon encountering nerve agents in solution.

Fig. 2A illustrates the fabrication steps involved in the preparation of FLA/silica–NH_2/Pt micromotors for the detection of nerve agents. The new micromotors were prepared by impregnation of FLA into silica microparticles using the incipient wetness technique[27] (refer to Experimental section) followed by asymmetric deposition (for the dynamic movement of micromotors) of Pt by sputtering (Fig. 2A). This technique allows the FLA solution to just wet the adsorbent and be completely adsorbed on solid silica–NH_2 particles.

Scanning electron microscopy (SEM) images of silica–NH_2 particle before and after the dye loading are shown in the ESI.† The surface of FLA coated silica particles displays a rough, shiny, and bright white morphology when compared to unmodified silica particles, indicating that the FLA molecules are adsorbed on the surface of silica–NH_2 microparticles. Energy dispersive spectroscopic (EDX) analysis of impregnated and un-impregnated samples qualitatively confirms the impregnation as indicated by the presence of the respective element in the EDX spectra (refer to ESI†). The presence of Janus micromotors is also confirmed by the corresponding EDX mapping of Pt and carbon displayed in Fig. 2C and D. Fig. 2E and F illustrate the initial movement of the dye coated micromotors in pure water and the movement after 5 minute propulsion, respectively. The tracking trajectories in Fig. 2E and F display the motion over a 5 s period, with an average speed of $\sim$145 μm s^{-1}.

To demonstrate the practical utility of the new micromotor-based fluorescent "*On–Off*" nerve-agent detection in environmental matrices, we investigated the ability to detect the sarin and soman simulants (Fig. S1, ESI†). In order to mimic the natural environment, experiments were carried out in water without buffer for the real time detection of nerve agents. Fig. 3 shows a FLA-coated silica–NH_2 particle that exhibits fluorescence counts of $\sim$40 000. Fig. 3B and C displays the comparative fluorescence intensity before and after FLA/silica–NH_2/Pt micromotors navigated a DCP contaminated solution (10^{-3} M), respectively. There is an instant fluorescence quenching of the moving micromotor compared to static particles that did not show any fluorescence quenching under the same conditions, even after 5 min of interaction (Fig. 3D and E). Fig. 3F shows the crucial role of the movement of micromotors in the contaminated solution for the rapid screening of nerve agents when compared to the static coated particles under similar conditions. The unique movement of multiple micromotors with bubble generation across the contaminated samples results in a continuous mixing (without external agitation), which increases the likelihood of collision with nerve agent and leads to an increase in the rate of reaction, with the concomitant fluorescence quenching within a minute, as per collision theory.[28] This dramatic fluorescence quenching is attributed to the reaction of reactive phosphonates with the –NH_2 group of

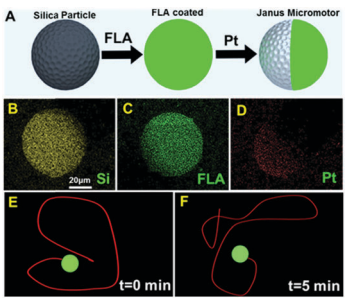

Fig. 2 (A) Schematic detailing the fabrication steps in the preparation of FLA/silica–NH_2/Pt micromotors; (B–D) energy-dispersive X-ray spectroscopy images illustrating the distribution of Si, dye and Pt; (E) tracking line (taken from ESI,† Video S1) illustrating the typical trajectories traveled by a micromotor over 5 second intervals at (E) t = 0 min and (F) t = 5 min.

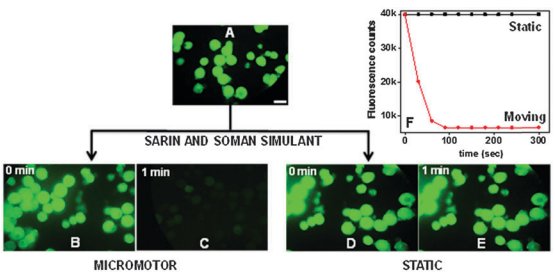

Fig. 3 (A) Fluorescent intensity of FLA coated silica–NH_2 particles; (B) fluorescent intensity of FLA/silica–NH_2/Pt micromotors before exposure to DCP; (C) after exposure; (D) fluorescent intensity of FLA/silica–NH_2/Pt static particles before exposure of DCP; (E) after exposure; and (F) graph showing the movement of micromotors leading to rapid quenching of fluorescence compared to static. Reaction conditions: conc. of DCP = 10^{-3} M, H_2O_2 (2%), SDS (1%), and 2 × 10^4 micromotors; λ_{ex}, 490 nm; λ_{em}, 510 nm. Scale bar 45 μm.

dye-coated micromotors which leads to the respective phosphoramide while releasing HCl which causes the interruption of the fluorophore's conjugation.[29] Unlike the fluorescence intensity increase expected from the formation of phosphoramide,[25] we observed a dramatic quenching in the fluorescence intensity of the FLPA adduct, attributed to the local decrease in pH due to the HCl release.

To expand the practical utility of the dye-coated micromotors towards diverse environmental applications, the fluorescence intensity of micromotors were also tested in sea water, pool water, and lake water. The resultant fluorescence intensity profile was consistent with that found in water experiments, which reflects its applicability in diverse natural environments. The specificity of this micromotor based detection was confirmed by monitoring the fluorescence with non-reactive phosphonates, such as dimethyl methyl phosphonate (DMMP; 10^{-3} M), and no fluorescence change was observed. The efficiency of the new micromotor-based *on-the-fly* fluorescent "*On–Off*" detection strongly depends on the concentration of nerve agents. Fig. 4A displays the time dependent quenching of FLA-coated micromotors with respect to varying DCP concentrations ranging from 10^{-1} to 10^{-6} M using a fixed number of micromotors. As expected, the fluorescence quenching is very fast (within a minute) for concentrations as low as 10^{-3} M DCP. Moreover, this micromotors based detection platform is able to sense concentrations as low as 10^{-6} M DCP within 3 minutes.

The detection efficiency at different concentrations of DCP with micromotor and static dye-coated particles was also compared (Fig. 4B). As expected, the reaction between the FLA-coated micromotors and the target DCP was very fast. For example, quenching of the motors was observed after only 120 s of interaction with a 10^{-4} M DCP contaminated solution. In contrast, when the contaminated solution is in quiescent conditions, the reaction between static FLA-coated silica particles and DCP is inefficient, thereby requiring around 30 min to exhibit a quenching of the fluorescence.

In order to optimize the density of micromotors for the rapid detection of 10^{-6} M DCP solution, different numbers of FLA-coated silica micromotors (1×10^4 to 2×10^4 micromotors per ml), were propelled in 600 μl contaminated solution for 3 min. It was found that an increase in the micromotor density increases the rate of CWA detection. Fig. S4 (ESI†) displays the effect of micromotor density on the detection rate (rapid fluorescence quenching) of DCP in a contaminated solution. We have also performed micromotor-based fluorescent enhancement detection of DCP in a phosphate buffer (pH 7.2) medium based on the conversion of dye in to phosphoramide. This resulted in a rapid and intense initial fluorescence increase in the presence of different DCP concentrations (Fig. S5, ESI†). However, this data illustrates that at longer times (>1.5 min) this enhancement may decay, depending on the DCP concentration. Such decrease is expected for this specific phosphoramide reaction since there is also a release of hydrochloric acid which can be partially neutralized by the buffer medium. At higher DCP concentrations ($>10^{-2}$ M), more acid production results in fluorescence quenching after the initial increase which may lead to false positive signals. Accordingly, practical detection applications based on the fluorescence enhancement should rely on the initial response in the buffer medium over the first 90 s. Fig. S6 (ESI†) shows the crucial role of the movement of micromotors in the buffer solution (pH 7.2) containing 10^{-3} M of DCP, compared to the static dye-coated particles under similar conditions. As expected, the fluorescence intensity drastically increases when compared to the static counterpart, reflecting the near instantaneous reaction of DCP with dye-coated micromotors due to continuous mixing associated with the micromotor movement. So, in both cases (buffer or non-buffer media) the micromotors lead to a greatly enhanced sensitivity compared to static systems. Interference studies were carried out in the presence of common volatile organic compounds, including ethanol, toluene, acetone, and isopropanol in order to demonstrate the applicability of the present methodology. As illustrated in Fig. S7 (ESI†), these organic compounds had a negligible effect upon the fluorescent signal, indicating effective discrimination against volatile organic compounds.

The greatly enhanced detection reflects the fluid mixing capability of the dye-coated micromotors. The experimentally observed rapid fluorescent detection achieved by the mobile micromotors, compared to static micromotors, can be attributed to and explained mathematically by three effects. First, the propulsion of mobile motors is able to keep them suspended and well dispersed in the solution. In contrast, the static motors settle to the bottom of the container, due to gravity, forming a densely packed aggregate. The mass-transfer model for the two systems provided in the ESI† shows that motors well dispersed in solution lead to significantly smaller diffusion mass-transfer resistance compared to sedimented motors; even without accounting for the continuous movement of the micromotors. This model estimates an enhancement of roughly $1 + (\pi Dt/4R^2)^{1/2}$ in the amount of analyte (DCP) reacted after time t at the surface of dispersed *versus* sedimented motors, where D is the diffusivity of the analyte in solution, R is the motor radius, and t is the time. Plugging in our determined estimates of DCP diffusivity and our micromotor size, one obtains a possible experimental enhancement due to micromotor suspension up to 25-fold during the first 10 minutes of motor activity. Second, the motion of the micromotors leads to convection-induced enhancement in the mass transfer of the analyte. In other words, the mobile motor leads to a larger

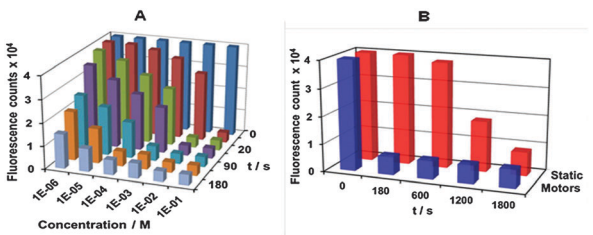

Fig. 4 Effect of inter-dependent parameters on the quenching of fluorescence intensity of FLA/silica–NH_2/Pt micromotors: (A) time dependent quenching of micromotors with different concentrations of DCP; and (B) comparison of fluorescent quenching with micromotor and static FLA-coated silica with 10^{-4} M DCP. Reaction conditions: H_2O_2 (2%), SDS (1%), λ_{ex}, 490 nm; λ_{em}, 510 nm.

number of collisions between the analyte and the motor surface, thereby enhancing the net rate of reaction. It can be shown that the additional enhancement in the flux arising from motor motion, on top of diffusion, is roughly given by $\sim 0.664 Re^{1/2} Sc^{1/3}$, where Re is the Reynolds number and Sc is the Schmidt number. Our calculations find this additional enhancement due to convection to be ~31% more than diffusion alone (see ESI†). Third, the continuous formation of bubbles during motor propulsion leads to improved mixing of the analyte in the solution, which is also expected to increase the transport of analyte to the surface of the motors. While the 44 fold-enhancement in surface flux due to this effect is difficult to estimate, we have previously shown that the generated bubbles significantly enhance the transport of tracer particles in the vicinity of the motors.[26] Thus, the combined effects of the propulsion of micromotors are critical to the rapid detection of the target analyte whereas static lead to slow rates of reaction and long operation time.[30] Similar enhancements in mass transport have been observed in other self-propelled systems.[18–20,30,31]

In conclusion, we have demonstrated the first example of a micromotor based fluorescent ''*On–Off*'' strategy for the rapid '*on-the-fly*' screening of sarin and soman related threats within seconds. The continuous mixing induced by the motion of multiple micromotors across a contaminated sample results in a greatly enhanced mass transport, and hence leads to increased rates of reaction between contaminated solution and micromotors when compared to static micromotor counterparts. The rapid micromotors based screening can be coupled to more elaborate fluorescence enhancement strategies to confirm nerve agent presence. The same reaction has also been performed in a buffer medium where the presence of the dye-coated micromotors led to a significantly pronounced response compared to static parts. Compared to common nerve agent detection methodologies, this micromotor-based screening methodology gives real time detection towards on-site measurements in many environmental matrices. Movement of the FLA-coated micromotors accelerates their ''on the fly'' real-time quenching of fluorescence upon contact with reactive nerve agents. The present study thus supports that the motion of micro/nanoscale motors and the corresponding fluid transport can notably improve the rapid and reliable detection of sarin and soman. We anticipate that the present micromotor-based fluorescent detection platform can be implemented practically and inspire further research in the field of micromotor-based sensing towards a broad range of chemical threats. The autonomous movement and built-in fluid mixing capability of dye-coated micromotors thus hold considerable promise for enhancing the detection power of a wide range of chemical sensing processes.

This project received support from the Defense Threat Reduction Agency-Joint Science and Technology Office for Chemical and Biological Defense (Grant no. HDTRA1-13-1-0002) and the UCSD Calit2 Strategic Research Opportunities (CSRO) program.

Notes and references

1 Y. C. Yang, *Acc. Chem. Res.*, 1999, **32**, 109–115.
2 W. Krutzsch and R. Trapp, *A commentary on the chemical weapons convention*, Martinus Nijhoff Publishers, London, 1994.
3 Organization for the Prohibition of Chemical Weapons. Proceedings, Convention on the Prohibition of the Development, Production, Stockpiling and Use of Chemical Weapons and on Their Destruction; Opened for Signature: Paris, France, 1993.
4 M. Ehrich, in *Encyclopedia of Toxicology*, ed. P. Wexler, Academic Press, San Diego, CA, 1998, p. 467.
5 F. R. Sidell and J. Borak, *Ann. Emerg. Med.*, 1992, **21**, 865–871.
6 T. C. Marrs, *Pharmacol. Ther.*, 1993, **58**, 51–66.
7 S. E. Letant and M. J. Sailer, *Adv. Mater.*, 2000, **12**, 355–359.
8 S. W. Zhang and T. Swager, *J. Am. Chem. Soc.*, 2003, **125**, 3420–3421.
9 (*a*) H. Sohn, S. E. Letant, M. J. Sailor and W. Trogler, *J. Am. Chem. Soc.*, 2000, **122**, 5399–5400; (*b*) J. Wang, M. Pumera, G. E. Collins and A. Mulchandani, *Anal. Chem.*, 2002, **74**, 6121–6125; (*c*) S. Jo, D. Kim, S. H. Son, Y. Kim and T. S. Lee, *ACS Appl. Mater. Interfaces*, 2014, **6**, 1330–1336; (*d*) J. Lee, S. Seo and J. Kim, *Adv. Funct. Mater.*, 2012, **22**, 1632–1638.
10 A. Barba-Bon, A. M. Costero, S. Gil, F. Sancenon and R. Martinez-Manez, *Chem. Commun.*, 2014, **50**, 13289–13291.
11 S. Han, Z. Xue, Z. Wang and T. B. Wen, *Chem. Commun.*, 2010, **46**, 8413–8415.
12 T. J. Dale and J. Rebek Jr., *J. Am. Chem. Soc.*, 2006, **128**, 4500–4501.
13 D. Patra, S. Sengupta, W. Duan, H. Zhang, R. Pavlick and A. Sen, *Nanoscale*, 2013, **5**, 1273–1283.
14 W. Gao, X. Feng, A. Pei, Y. Gu, J. Li and J. Wang, *Nanoscale*, 2013, **5**, 4696–4700.
15 E. Morales-Narváez, M. Guix, M. Medina-Sánchez, C. C. Mayorga-Martinez and A. Merkoçi, *Small*, 2014, **10**, 2542–2548.
16 W. Gao and J. Wang, *ACS Nano*, 2014, **8**, 3170–3180.
17 (*a*) D. Kagan, S. Campuzano, S. Balasubramanian, F. Kuralay, G. Flechsig and J. Wang, *Nano Lett.*, 2011, **11**, 2083–2087; (*b*) J. G. S. Moo, H. Wang, G. Zhao and M. Pumera, *Chem. – Eur. J.*, 2014, **20**, 4292–4296.
18 J. Orozco, G. Cheng, D. Vilela, S. Sattayasamitsathit, R. Vazquez-Duhalt, G. Valdes-Ramirez, O. S. Pak, A. Escarpa, C. Kan and J. Wang, *Angew. Chem., Int. Ed.*, 2013, **52**, 13276–13279.
19 (*a*) J. Li, V. V. Singh, S. Sattayasamitsathit, J. Orozco, K. Kaufmann, R. Dong, W. Gao, B. Jurado-Sanchez, Y. Fedorak and J. Wang, *ACS Nano*, 2014, **8**, 11118–11125; (*b*) V. V. Singh, B. Jurado-Sánchez, S. Sattayasamitsathit, J. Orozco, J. Li, M. Galarnyk, Y. Fedorak and J. Wang, *Adv. Funct. Mater.*, 2015, **25**, 2147–2155.
20 B. Jurado-Sanchez, S. Sattayasamitsathit, W. Gao, L. Santos, Y. Fedorak, V. V. Singh, J. Orozco, M. Galarnyk and J. Wang, *Small*, 2015, **11**, 499–506.
21 C. J. Cumming, C. Aker, M. Fisher, M. Fox, M. J. Grone, D. Reust, M. G. Rockley, T. M. Swager, E. Tower and V. William, *IEEE Trans. Geosci. Remote Sens.*, 2001, **39**, 1119–1128.
22 A. Rana and P. K. Panda, *RSC Adv.*, 2012, **2**, 12164–12168.
23 J. Du, M. Liu, X. Lou, T. Zhao, Z. Wang, Y. Xue, J. Zhao and Y. Xu, *Anal. Chem.*, 2012, **84**, 8060–8066.
24 (*a*) L. A. Saari and W. R. Seitz, *Anal. Chem.*, 1982, **54**, 821–823; (*b*) Z. Zhang, Y. Zhang, W. Ma, R. Russell, Z. M. Shakhsher, C. L. Grant, W. R. Seitz and D. C. Sundberg, *Anal. Chem.*, 1989, **61**, 202–205; (*c*) H. D. Duong, O. J. Sohn, H. T. Lam and J. I. Rhee, *Microchem. J.*, 2006, **84**, 50–55.
25 S. B. Nagale, T. Sternfeld and D. R. Walt, *J. Am. Chem. Soc.*, 2006, **128**, 5041–5048.
26 J. Orozco, B. Jurado-Sánchez, G. Wagner, W. Gao, R. Vazquez-Duhalt, S. Sattayasamitsathit, M. Galarnyk, A. Cortes, D. Saintillan and J. Wang, *Langmuir*, 2014, **30**, 5082–5087.
27 A. Saxena, A. K. Srivastava, B. Singh and A. Goyal, *J. Hazard. Mater.*, 2012, **211**, 226–232.
28 A. K. Dutt and S. C. Miller, *J. Phys. Chem.*, 1993, **97**, 10059–10063.
29 L. Y. Ma, H. Y. Wang, H. Xie and L. X. Xu, *Spectrochim. Acta, Part A*, 2004, **60**, 1865–1872.
30 P. Garstecki, M. A. Fischbach and G. M. Whitesides, *Appl. Phys. Lett.*, 2005, **86**, 244108.
31 G. Mico, T. E. Mallouk, T. Darnige, M. Hoyos, J. Dauchet, R. Soto, Y. Wang, A. Rousselet and E. Clement, *Phys. Rev. Lett.*, 2011, **106**, 048102.